

Spin-configuration-related ferromagnetic resonance in nickel nanowire array

This article has been downloaded from IOPscience. Please scroll down to see the full text article.

2005 J. Phys.: Condens. Matter 17 3637

(<http://iopscience.iop.org/0953-8984/17/23/015>)

View [the table of contents for this issue](#), or go to the [journal homepage](#) for more

Download details:

IP Address: 129.252.86.83

The article was downloaded on 28/05/2010 at 04:59

Please note that [terms and conditions apply](#).

Spin-configuration-related ferromagnetic resonance in nickel nanowire array

Tao Li^{1,4}, Yunxia Sui², Zhigao Huang³, Shaoguang Yang¹, Benxi Gu¹ and Youwei Du¹

¹ National Laboratory of Solid State Microstructures, Nanjing University, Nanjing 210093, People's Republic of China

² Center of Material Analysis, Nanjing University, Nanjing 210093, People's Republic of China

³ Physics Department, Fujian Normal University, Fuzhou 350007, People's Republic of China

E-mail: litao@nju.org.cn

Received 14 March 2005, in final form 5 May 2005

Published 27 May 2005

Online at stacks.iop.org/JPhysCM/17/3637

Abstract

The angular dependence of specific precession modes of an Ni nanowire array in the magnetization process was thoroughly investigated by ferromagnetic resonance. Compared with the uniform precession mode in near-saturated states, additional resonance was observed at low applied fields when the field orientation diverged from the wire axis. The origin of such a low-field resonance is discussed in detail in the transverse magnetization case. The particular resonances were considered from the spin precession in remanent longitudinal domains in the unsaturated states of the nanowires, which gave strong experimental evidence of a nucleation mode in the magnetization process of the nanowire array.

(Some figures in this article are in colour only in the electronic version)

1. Introduction

Arrays of ferromagnetic submicro- or nanostructures have recently attracted much interest for the wide potential applications in data storage, magnetic sensors and microwave devices, and much interesting physics is indicated in such confined magnetic systems as well. Since the preparation and static properties of these magnetic nanostructures have been intensively studied [1–3], many researchers have turned their focus to the spin dynamics, which is of fundamental importance in evaluating the timescale of the magnetization reversal process [4–9]. A ferromagnetic nanowire array, electrodeposited in certain templates, provides a suitable system for studies of the static and dynamic magnetic properties due to controllable and reproducible characteristics and properties. Many theoretical calculations based on the cylinder model have provided the behaviours of the domains in the anisotropic magnetization process

⁴ Author to whom any correspondence should be addressed.

in detail [10–12]. More recently, spin wave modes and microwave response have attracted much attention both in experiments and theory [13–16]. Wang *et al* also found the spin wave quantization in the nickel nanowire array [17].

Ferromagnetic resonance (FMR) is a classical experimental method in the field of magnetism, which can reveal a lot of information such as the magnetization, surface and volume anisotropies, g factor, damping, etc. Most of the previous works about the spin precession and spin wave excitations in the nanowires were in the magnetic saturation states. FMR studies of Ebels revealed a good match of the angular dependence of the resonance field by the uniform precession mode in saturated Ni wire array system [13]. Magnetostatic coupling among the nanowires in the array was illustrated as an effective anisotropy field H_{eff} . Additionally, a low-field peak was observed and considered as the exchange/dipole spin wave modes, which was also investigated theoretically by Arias and Mills [14, 16].

In the present work, we used FMR to study the dynamic behaviour of the Ni nanowire array at a considerably lower frequency (9.7 GHz, X band). In this band, the resonance occurred in a certain external field, which may not make the wire array saturated completely. Two discrete peaks were clearly observed as the external bias field orientation diverged far from the nanowire axis. A uniform precession mode was used to fit the high-field resonance (HFR) peak, resulting in a considerable discrepancy. The low-field resonance (LFR) depended remarkably on the direction of microwave pumping field h_{rf} . If the discrepancy of the HFR field can be attributed to spin dispersion in the near-saturated states, the emergence of LFR in transverse or other large-angle magnetization seems more intricate. Since magnetization and its reversal process is an important problem in the research on nanomagnetism, abundant works based on micromagnetic calculation were carried out to investigate the reversal mechanism and the complicated domain structures in the nanowires and wire array system [10–12]. As well as the theoretical efforts, experiments were also devised, with the same purpose. However, unfortunately, few experimental approaches can obtain the elaborate spin configuration and dynamics, suffering from only average information provided in the measurements. Although some phenomenological models (i.e. buckling, curling, chain of crystals etc) were constructed to explain some particular features observed, such as enhanced squareness of the hysteresis loop, enlarged cohesive field, and so on [18], they could not offer convincing evidence of the domain configuration. In the present study, with the aid of orientation-dependent FMR, we elaborated the specific resonances of confined spin in such a nanowire array system, and experimentally explained the origin of a low-field resonance in the transverse magnetization process. Our investigation provides an explicit confirmation of the nucleation model in the magnetization process of the nanowires.

2. Experimental details

The nickel nanowire arrays embedded in the porous anodic alumina (PAA) membrane were prepared by the electrodeposition method as described elsewhere [19, 20]. In this experiment, two samples with different wire diameters were fabricated by the corresponding characteristic PAA membranes. Transmission electron microscope (TEM) observations revealed that the wires have a length of the order of 50 μm , and the wire diameters are about 20 and 35 nm respectively for the two samples. Interwire distance was kept at about 70 nm for both samples, determined by the nanopore arrangement of the PAA membrane, which was also characterized by TEM.

Magnetization loops of the samples were measured by vibrating sample magnetometer (VSM) in parallel and vertical directions, respectively. In agreement with previous reports [1, 19], the nanowire arrays manifest strong shape anisotropy due to their high aspect

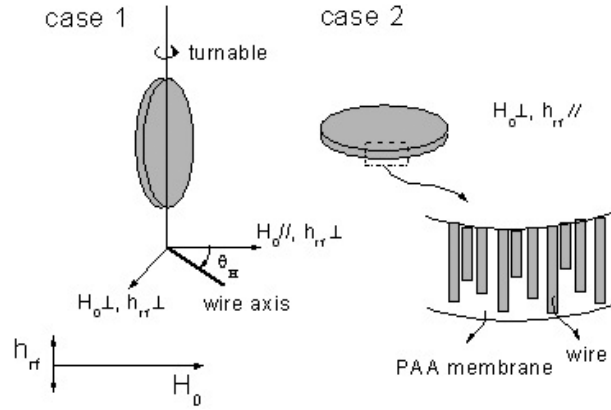


Figure 1. A schematic diagram of the FMR measurements, showing two different sample positions. H_0 is the applied bias field and h_{rf} is the microwave pumping field.

ratio. In the transverse magnetization case, which will be intensively investigated in the later FMR discussion, the saturated fields for the 20 nm and 35 nm diameter samples are about 5000 and 4000 Oe respectively. In addition, magnetostatic coupling among the wires may provide a considerable contribution, which is exhibited in the FMR investigation as well.

An electron paramagnetic resonance spectrometer (Bruker, EMX-10/12) was employed in the FMR measurements. Figure 1 is a schematic diagram, showing two different sample locations. In case 1 the angle (θ_H) between applied bias field H_0 and the wire axis can be adjusted from 0° to 90° with a perpendicular microwave pumping field h_{rf} , while h_{rf} is kept parallel to the wire axis and H_0 is perpendicular to the wires in case 2. All of the measurements were performed at the frequency of 9.7 GHz (X band) and the angular dependence of the applied bias field (θ_H from 0° to 90°) in case 1 was investigated in detail.

3. Result and discussions

3.1. Angular dependent resonance field

A sequence of FMR derivative spectra for a 20 nm Ni wire array at 9.7 GHz is shown in figure 2 with the wire orientation from parallel ($H \parallel$) to perpendicular ($H \perp$) to the bias field. It can be clearly observed that with the angle θ_H increasing, the resonance changes from one relatively narrow peak to two weak broad peaks and the high resonance field H_{res} keeps increasing. Similar results are obtained in the other 35 nm diameter sample with a smaller resonance field gap between the parallel and perpendicular field orientations. By integrating the derivative spectra to its original resonance absorption peaks, we obtained the HFR fields in sequence, which were presupposed as the uniform precession mode temporarily. The angular dependence of the resonance field (H_{res} versus θ_H) is plotted in figure 3. The two kinds of symbols represent two sample diameters. From the data, the different porosity caused by different diameter of the Ni wire implies remarkable importance in the FMR, which was concluded as the dipolar interaction among the wires [21].

According to the equation of spin motion $d\mathbf{M}/dt = \gamma(\mathbf{M} \times \mathbf{H}_{eff})$, where $\gamma = g\mu_B/\hbar$ (μ_B is the Bohr magnetic moment), the gyromagnetic ratio. The resonant frequency can be obtained as [13, 21]

$$\frac{\omega}{\gamma} = [(H_{eff} \cos 2\theta_0 + H_0 \cos(\theta_0 - \theta_H))(H_{eff} \cos^2 \theta_0 + H_0 \cos(\theta_0 - \theta_H))]^{1/2} \quad (1)$$

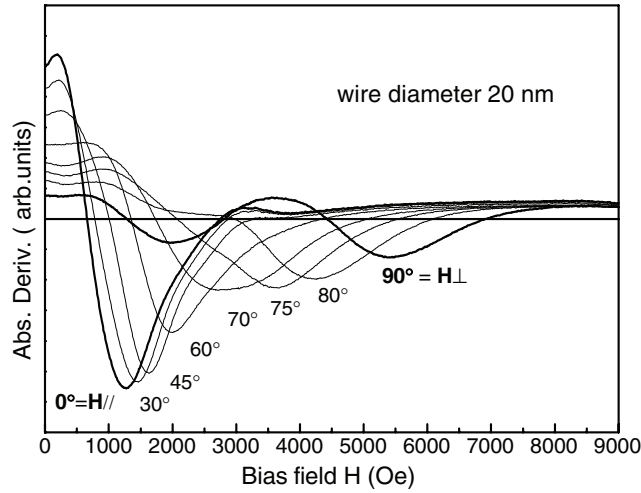


Figure 2. A sequence of FMR derivative spectra for 20 nm Ni wire array at 9.7 GHz with the wire orientation from parallel ($H \parallel$) to perpendicular ($H \perp$) to the bias field.

where H_{eff} is an effective uniaxial field along the wire axis, which mainly contains two parts: the shape anisotropy wire itself and the dipolar interaction among wires; θ_0 and θ_H are the equilibrium angle of the magnetization M and applied field (H_0) direction angle respectively.

In the phenomenological approximation, the dipolar interaction is expressed as a uniaxial mean field H_U , which favours an easy axis perpendicular to the wires. Considering the high aspect ratio of the nanowires, the effective field taken from the shape demagnetization is $2\pi M_s$. Thus the total anisotropy field is written as $H_{\text{eff}} = 2\pi M_s - H_U$. In such a wire array system, the uniaxial mean field can be considered proportional to the porosity $P = \frac{2\pi}{\sqrt{3}} \left(\frac{R}{d}\right)^2$ [21], where $R = D/2$, the radius of the wire, and d is the inter-wire distance. Then we have

$$H_{\text{eff}} = 2\pi M_s - 6\pi M_s P. \quad (2)$$

Substituting equation (2) into (1), we numerically calculated the resonant field (H_0) corresponding to the angle of the bias field (θ_H). The parameters used for Ni are $g = 2.21$, $\gamma' = \gamma/(2\pi) = 3.09 \text{ MHz Oe}^{-1}$ and $M_s = 485 \text{ emu g}^{-1}$, and the FMR frequency $f = \omega/(2\pi) = 9.78 \text{ GHz}$. The theoretical results are shown as curves in figure 3(a), which reveal the fits in the low and high θ_H region rather better than in the angle region 50° – 80° both for the 20 nm and 35 nm diameter samples. Here we did not try to make a best fit to the experimental data by alternating the g factor or packing density (P) in order not to cover up some special physical facts. The angle difference between the applied field (θ_H) and the equilibrium state (θ_0) was also calculated as a function of θ_H , shown in figure 3(b). It is clearly seen that the value of discrepancy in the 20 nm diameter sample is much larger than the 35 nm diameter one, and their maximum location lowers in angle value with increasing diameter. The tendency of change of the angle difference is in agreement with that of the discrepancy as illustrated in figure 3(b).

Our calculated results demonstrate an obvious relationship between discrepancies and the angle differences; in general, the bigger the angle difference, the larger the discrepancy. But even if the wire is not completely saturated, equation (1) is still adaptive because it permits the difference of θ_0 and θ_H . Then there must be something incorrect with our model. The greatest problem may come from the fact that the whole wire cannot offer only one θ_0 of the spins.

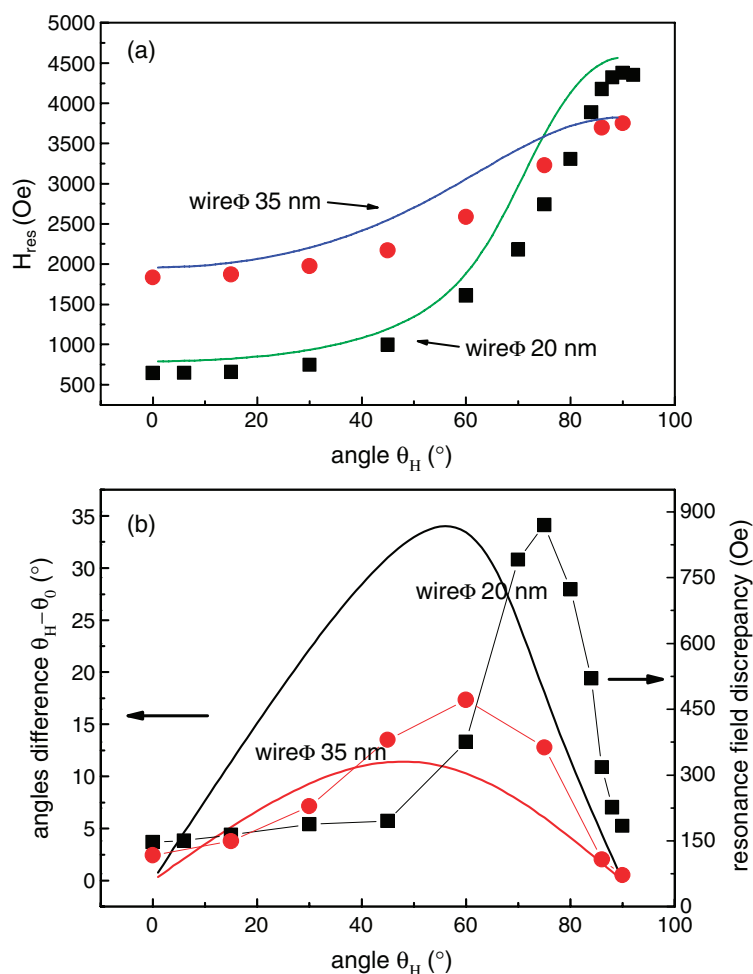


Figure 3. (a) Angular dependence of the high resonance field; the symbols are the experimental data and the lines are theoretical results both for the 20 nm and 35 nm diameter samples. (b) The angle difference ($\theta_H - \theta_0$) and the discrepancy of the theoretical and experimental resonance field as functions of the applied field orientation θ_H .

Factually, quite different from the uniform rotation, the spin arrangements should vary spatially inside the wires in magnetization or its reversal process. Many theoretical simulations have presented various domain structures in the nanowire system [10–12, 22]. The effective field is considerably diversified inside the wire, which cannot be considered as a mean magnetization in a certain direction when we study the spin precessions. Different from the study of Ebels *et al* [13], in which the resonance in higher frequencies (K band and Q band) was intensively investigated and the uniform precession mode fitted the experimental data well, our results reveal the remarkable effect on the spin configuration by the stray fields inside the wires. The inhomogeneous internal fields in the near-saturated states actually result in the discrepancy in resonance fields between the theoretical and experimental. Undoubtedly, the broadened line-width as the angle θ_H increase is another effect of the low-dispersion spins caused by the stray fields in near-saturated states. In the following, we will discuss the additional resonance peak at the lower field in the high- θ_H region.

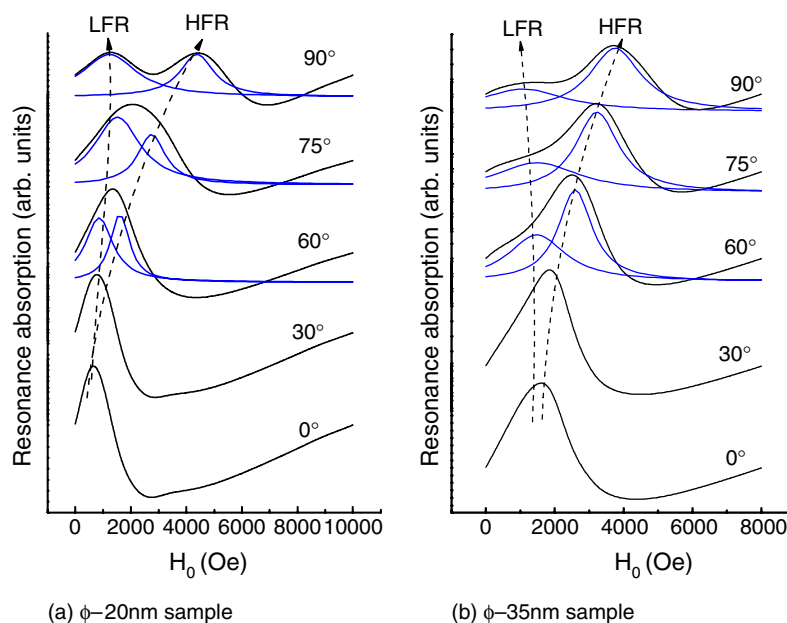


Figure 4. The deconvolved resonance peaks from the derivation spectra of both 20 nm and 35 nm diameter samples in different field orientations.

3.2. Low-field additional resonance

From the above discussions, we have realized the importance of the stray field inside the nanowires caused by complex domain structures when they are not completely saturated. Now we will demonstrate another very important experimental phenomenon, which provides convincing information to uncover the spin arrangements in the transverse magnetization process.

Figure 4 shows the deconvolved resonance peaks from the derivation spectra of both 20 nm and 35 nm diameter samples in different field orientations. Two resonance peaks can be clearly observed in the large-angle region: high-field resonance (HFR) and low-field resonance (LFR). For simplification, the HFR peaks are still regarded as the uniform precession mode, although the system is only near saturation in most cases. However, the additional low-field peak seems less explicable. From figure 4, the two peaks departed distinguishably as the angle of the field direction became larger than 60° in both samples; and the low-field peak positions do not change greatly. More carefully, it is observed that the intensity of the LFR peaks of the 35 nm sample is much weaker than that of the 20 nm ones. To explore the origin of this LFR, we mainly investigated the transverse magnetization case, in which the additional peak is relatively strong and the spin configuration has also been discussed in the previous reports [10].

According to the Hertel simulation, the remanent state of a nanowire is not unique in the transverse case. Two different zero-field states were presented after the wire was technically saturated perpendicular to its axis: head on domain wall with the domain orientation towards and away from the wall, as shown in figure 5 [10]. No matter which case occurs, it is conclusive that most spins are along the wire axis in the remanent state with an 180° domain wall. This domain wall can also be regarded as a centre transverse-spin domain (TSD) with two 90° domain walls. With the transverse field increase, the centre TSD expands by the propagation of two domain walls, while those spins far from the domain walls should still keep in a longitudinal

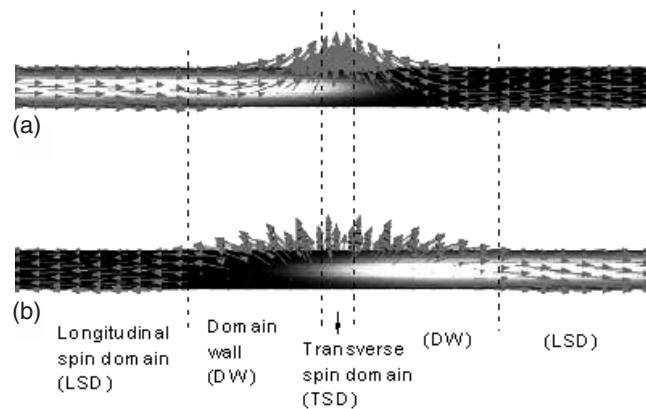


Figure 5. Scheme of two different zero-field states after the wire was technically saturated perpendicular to its hard axis: head on domain wall with the domain orientation (a) towards and (b) away from the wall. Another definition of the domains is drawn schematically with two 90° domain walls.

orientation before rearrangement. Until the applied field is strong enough it can exert all the spins to orient perpendicular to the wires, where a saturated state is reached. The LFR truly occurs in a middle state with many spins still along the wire axis far from saturate. Although it is premature to determine the origin of the LFR, it might be suggested that the LFR is related with the remained longitudinal spins in the unsaturated states. Furthermore, by comparing LFR of the two samples, it appears reasonable that the weaker LFR intensity of the 35 nm diameter sample should attribute to the weaker anisotropy. Because from equation (2) we can see that the larger packing density, the smaller effective field, and thus the weaker ability of the system to confine the spins arranged longitudinally. Then the remained longitudinal spins in 35 nm sample are much fewer than the 20 nm sample in a certain small external field. From this point of view, a hypothesis that the LFR comes from the precessions of the remaining longitudinal spins is quite convincing. It should be mentioned that the experimental system of our Ni wire array is far from homogenous as theoretically assumed, featuring polycrystallinity and imperfections. Although these facts affect the magnetic behaviour of the array considerably, especially in the parallel magnetization case [18], the substantial magnetization mechanism in the transverse case is the same as the micromagnetism simulated by considering there are multiple initial nuclei of TSD located at the defects or grain boundaries of the wires. As the nanowires have very high aspect ratio, whether there is a single nucleus or multiple ones in the initial magnetization is not important in a qualitative interpretation. Then even for a polycrystalline system, the hypothesis about the origin of the LFR is still plausible.

A further experimental result of FMR with a parallel pumping field confirms our hypothesis. Two FMR spectra with different pumping field directions (drawn schematically in figure 1) are shown in figure 6 and the inset displays the resonance absorption peaks of the two cases. From the figure we can see that although they are in the same bias field ($H_0 \perp$ wire), the resonance behaviours are quite different. There are two peaks in perpendicular pumping, while only one in parallel pumping. According to the spin dynamics, the resonance is orientation dependent, which only occurs when the spin orients perpendicular to the microwave pumping field. The disappearance of the LFR in the parallel pumping case indicates that the LFR in the perpendicular pumping case belongs to the precession of the longitudinal spins. This is in good agreement with the hypothesis we have made.

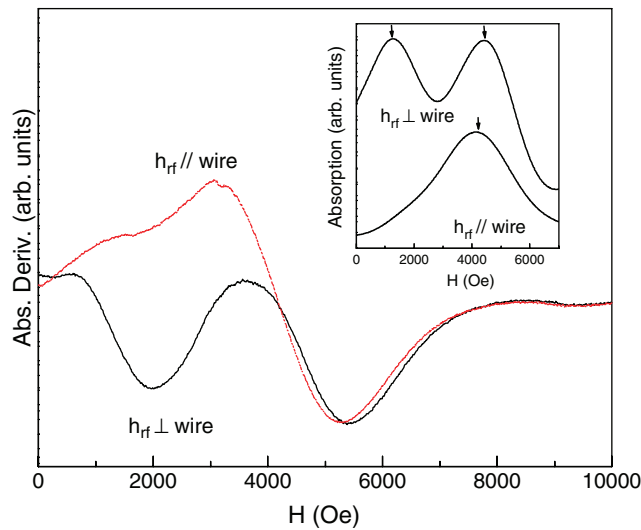


Figure 6. Two resonance derivative spectra with different pumping field directions, while the applied fields are both perpendicular to the wire axis. Inset is the integrated resonance absorption spectra.

Physically, to answer the question of why the LFR actually takes place in a certain perpendicular applied field, a phenomenological explanation is presented here. As is well known, the resonance takes place when the pumping microwave frequency matches the spin precession determined by the effective field around it. In the unsaturated states for our nanowire system, before being involved in the domain walls, these remaining longitudinal spins may undergo a changing longitudinal effective field, which is a composition of the external transverse field, the canting stray field formed by the complex domain structure and the dipolar field from surrounding wires. In fact, the matching condition of the LFR may not be strict due to its broad line-width, which means resonance occurs from a certain broad field region around the intrinsic resonance field the spin precession requires. The closer to the specific field, the more strongly the resonance occurs. At the present frequency (9.7 GHz), the intrinsic resonance field of Ni is about 3.17 kOe, which is very near to ideal Ni wires' demagnetization field H_d (~ 3.05 kOe). According to the former effective field formation equation (2), the dipolar field of interacting wires contributes a negative part ($-6\pi M_s P$) to H_{eff} in the initial longitudinal spin arranged states. When the transverse external field is added, complex domains appear in the surrounding wires as well, which decrease the negative contribution and make the effective field of the longitudinal spins in object-wire closer to its H_d , which is near to the resonance field. Thus the increasing external field will eventually make the resonance condition matches, resulting in the appearance of the LFR. Although it should appeal to the specific micromagnetic calculation to reveal the most detailed dynamic behaviours of the spins in such a nanowire system, our experimental results phenomenologically explained the origin of the LFR and provided clear physical pictures in magnetization process of nanowire array system confirming the existence of the domain motion as the simulation predicted.

4. Conclusion

From FMR results of the Ni nanowire array and discussions, we revealed a close relationship between the magnetic resonance and the particular spin configurations in magnetization

process. Both the angular dependence and the additional LFR reveal the existence of the complicated domain structure in unsaturated states of the wires, indicating the incorrectness of the uniform rotation model in the magnetization process. In the meantime, this affirms the validation of the micromagnetic simulation about the domain type and domain motion with strong experimental evidence. This work has presented a phenomenological explanation of the particular FMRs caused by specific spin configurations in the nanowire array system; theoretical work can go further to realize more detailed information on the confined spins.

As the cooperation of the magnon and microwave is a fascinating topic in nanomagnetism research, our results provide important information about the particular effects caused by the strong anisotropies. This is not only of great scientific importance in realizing the spin dynamics in the confined system but also very useful in designating and fabricating nanomagnetic apparatus and microwave devices.

Acknowledgments

This work is supported by the Natural Science Foundation of Jiangsu Province (grant No BK2001404) and a National Key Project of Fundamental Research (973, No G1999064508).

References

- [1] Sellmyer D J, Zheng M and Skomski R 2001 *J. Phys.: Condens. Matter* **13** R433
- [2] Skomski R 2003 *J. Phys.: Condens. Matter* **15** R841
- [3] Martíá J I, Nogués J, Liu K, Vicente J L and Schullerc I K 2003 *J. Magn. Magn. Mater.* **256** 449
- [4] Mathieu C, Jorzick J, Frank A, Demokritov S O, Slavin A N, Hillebrands B, Bartenlian B, Chappert C, Decanini D, Rousseaux F and Cambriil E 1998 *Phys. Rev. Lett.* **81** 3968
- [5] Ercole A, Adeyeye A O, Bland J A C and Hasko D G 1998 *Phys. Rev. B* **58** 345
- [6] Jorzick J, Demokritov S O, Mathieu C, Hillebrands B, Bartenlian B, Chappert C, Rousseaux F and Slavin A N 1999 *Phys. Rev. B* **60** 15194
- [7] Gérardin O, Gall H L, Donahue M J and Vukadinovic N 2001 *J. Appl. Phys.* **89** 7012
- [8] Jung S, Ketterson J B and Chandrasekhar V 2002 *Phys. Rev. B* **66** 132405
- [9] Skomski R, Chipara M and Sellmyer D J 2003 *J. Appl. Phys.* **93** 7604
- [10] Hertel R 2001 *J. Appl. Phys.* **90** 5752
- [11] Forster H, Schrefl T, Suess D, Scholz W, Tsiantos V, Dittrich R and Fidler J 2002 *J. Appl. Phys.* **91** 6914
- [12] Wieser R, Nowak U and Usadel K D 2004 *Phys. Rev. B* **69** 064401
- [13] Ebels U, Duvail J L, Wigen P E, Piraux L, Buda L D and Ounadjela K 2001 *Phys. Rev. B* **64** 144421
- [14] Arias R and Mills D L 2001 *Phys. Rev. B* **63** 134439
- [15] Chipara M I, Skomski R and Sellmyer D J 2002 *J. Magn. Magn. Mater.* **249** 246
- [16] Arias R and Mills D L 2003 *Phys. Rev. B* **67** 094423
- [17] Wang Z K, Kuok M H, Ng S C, Lockwood D J, Cottam M G, Nielsch K, Wehrspohn R B and Gösele U 2002 *Phys. Rev. Lett.* **89** 027201
- [18] Chen W, Tang S L, Lu M and Du Y W 2003 *J. Phys.: Condens. Matter* **15** 4623
Tang S L, Chen W, Lu M, Yang S G, Zhang F M and Du Y W 2004 *Chem. Phys. Lett.* **384** 1–4
- [19] Zheng M, Menon L, Zeng H, Liu Y, Bandyopadhyay S, Kirby R D and Sellmyer D J 2000 *Phys. Rev. B* **62** 12282
- [20] Zheng M, Skomski R, Liu Y and Sellmyer D J 2000 *J. Phys.: Condens. Matter* **12** 497
- [21] Encinas-Oropesa A, Demand M, Piraux L, Huynen I and Ebels U 2001 *Phys. Rev. B* **63** 104415
- [22] Hinzke D and Nowak U 2000 *J. Magn. Magn. Mater.* **221** 365